A New Coupling Network Topology for mm-Wave Biomimetic Antenna Arrays

Patrik Grüner[#1], David Schmucker[#], Christian Waldschmidt[#]
[#]Institute of Microwave Engineering, Ulm University, Germany
[1]pgruener@ieee.org

***Abstract* — Biomimetic antenna arrays (BMAAs) are used to improve the angle estimation capabilities of compact antenna systems by mimicking the hearing system of an insect. The key component of the antenna system is the biomimetic coupling network. Recent works propose the use of transformers for this purpose, but these are difficult to realize especially in the mm-wave range. In this paper, a new topology for the biomimetic coupling network based on rat-race couplers is proposed and a straightforward design process is given. A prototype antenna is designed, fabricated, and measured showing an excellent match between theory and measurement.**

***Keywords* — Biomimetic antenna array, biomimetic coupling network, direction-of-arrival estimation, rat-race coupler.**

I. Introduction

Biomimetic antenna arrays (BMAAs) were introduced recently as a concept to design antenna arrays with improved spatial resolution and improve the angle estimation capabilities of very compact direction finding systems or radars. They are composed of a conventional antenna array followed by a biomimetic coupling network. This coupling network is the key component of the BMAA and mimics the dynamical properties of the hearing system of the fly *Ormia ochracea* [1], [2]. It is usually composed of passive components and leads to an increased phase progression between the antenna elements for a certain angular range compared to an uncoupled array. The trade-off is a loss in output power. Recent implementations showed BMAAs for enhancing signals originating from directions around boresight [2], [3] as well as for off-boresight directions [4]. The biomimetic coupling networks were realized using lumped elements or microstrip lines. Other coupling networks were designed to maximize output power extraction [5] or improve the bandwidth by using active components [6], [7]. All of the mentioned topologies rely on a strong mutual coupling between the antenna elements.

A generalized electrical model of the BMAA that separates the biomimetic coupling from the antenna mutual coupling was presented in [8], enabling the use of basically every type of antenna element. The biomimetic coupling network in this generalized model contains a transformer and other passive components to modify the coupling amplitude and phase.

This paper takes up the working principle of the generalized model in [8] and presents a completely new topology for the biomimetic coupling network based on rat-race couplers. No transformer is necessary in the presented topology, simplifying the use especially in the mm-wave frequency range. The straightforward design enables an easy design process.

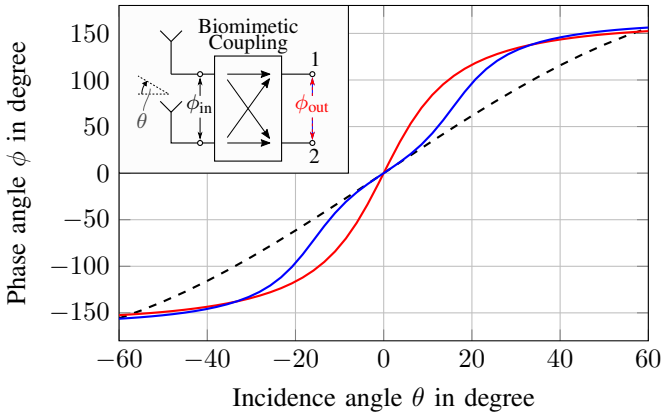

Fig. 1. Principal output phase difference ϕ_{out} of a biomimetic antenna array (BMAA) optimized for boresight (——) and off-boresight (——) applications. For comparison, the output phase difference (ϕ_{in}) of the uncoupled antenna array (- - -) is given [8].

II. Biomimetic Antenna Arrays

Fig. 1 shows the principle building blocks as well as characteristic phase differences of a BMAA. A plane wave impinging from an angle θ leads to a phase difference ϕ_{in} at the antenna base. Due to the biomimetic coupling, an increased phase difference ϕ_{out} is measured at the output of the BMAA.

Three parameters have been introduced so far to describe the BMAA on a system level: the phase gain η, the off-boresight factor ξ, and the normalized output power L_{out}. The increase in phase sensitivity in boresight direction, i. e., the steepness of the curve in Fig. 1 for $\theta = 0°$, is quantified by the phase gain η. It is defined as

$$\eta = \left.\frac{\mathrm{d}\phi_{out}(\theta)}{\mathrm{d}\theta}\right|_{\theta=0} \Big/ \left.\frac{\mathrm{d}\phi_{in}(\theta)}{\mathrm{d}\theta}\right|_{\theta=0}, \tag{1}$$

where $\phi_{out}(\theta)$ and $\phi_{in}(\theta)$ are the phase differences between the antenna ports with respect to the incidence angle θ of a BMAA and a conventional antenna with identical layout but without biomimetic coupling network, respectively.

The characteristic of ϕ_{out} can be modified by the biomimetic coupling network to account for target angles off the boresight region (cf. (——) in Fig. 1). This behavior is

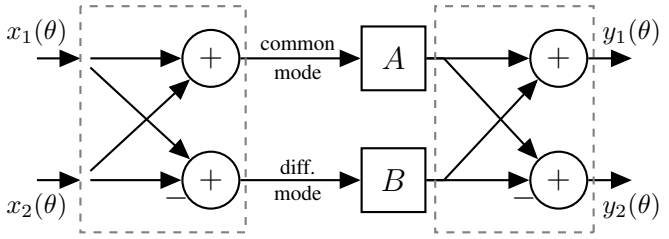

Fig. 2. Signal flow chart representation of the biomimetic coupling network with inputs $x_n(\theta)$, outputs $y_n(\theta)$, and scaling factors A and B (from [8]).

quantified by the off-boresight factor ξ, which is an indicator of how far the point of maximum sensitivity of ϕ_{out} is shifted away from the boresight direction. Its definition is given in [4].

The normalized output power L_{out} quantifies the loss in output power. It is calculated from the output power $P_{\text{out,BMAA}}$ of the BMAA normalized to the output power $P_{\text{out,conv.}}$ of a comparable conventional array as follows:

$$L_{\text{out}} = \frac{P_{\text{out,BMAA}}}{P_{\text{out,conv.}}} \,. \tag{2}$$

III. Proposed Coupling Network Topology

Starting from the generalized electrical model of the BMAA presented in [8] a new topology of the biomimetic coupling network is proposed. In that paper, the working principle of the biomimetic coupling was identified and a signal flow chart was developed showing the main signal paths in the biomimetic coupling network, cf. Fig. 2. The impinging signals at the antennas are modeled by two signals x_1 and x_2 with the same amplitude A_0. However, the phases of x_1 and x_2 differ according to

$$\arg(x_2) - \arg(x_1) = kd\sin\theta = 2\alpha \,, \tag{3}$$

where $k = 2\pi/\lambda$ is the wave number in free space, λ is the wavelength, d is the spacing of the two antenna elements, and θ is the angle of the impinging wave relative to the boresight direction. The sum of the two input signals (referred to as *common mode*) is multiplied by a complex factor A whereas the difference between x_1 and x_2 (referred to as *differential mode*) is scaled by a different complex factor B. Afterwards, the scaled signals of the common and differential mode are summed up or subtracted from each other forming the output signals y_1 and y_2, respectively.

A fully functional biomimetic coupling network was already proposed in [8]. However, the network required the use of a transformer whose design is quite complex, especially in the mm-wave domain. In this work, a new coupling network topology is proposed based on the flow chart shown in Fig. 2. The addition and subtraction of signals (cf. dashed gray boxes in Fig. 2) is supposed to be achieved by using two rat-race couplers. The inputs to the first rat-race coupler are the antenna signals x_1 and x_2. The sum port of the rat-race forms the common mode signal, whereas the difference port forms the differential mode signal. After the scaling with A and B, the second rat-race coupler is used to obtain the output signal y_1 via the sum port and y_2 via the difference port. The complex scaling between the two rat-race couplers can, e. g., be achieved by using passive components like attenuators, phase shifters, and filters or active components like varactors and amplifiers.

From the signal flow graph in Fig. 2 the following relations between the input and output signals are obtained assuming ideal rat-race couplers:

$$y_1 = -\frac{1}{2}\left(A(x_1 + x_2) + B(x_1 - x_2)\right) \tag{4}$$

$$y_2 = -\frac{1}{2}\left(A(x_1 + x_2) - B(x_1 - x_2)\right) \,. \tag{5}$$

With the input signals $x_1 = A_0\,\mathrm{e}^{-\mathrm{j}\alpha}$ and $x_2 = A_0\,\mathrm{e}^{\mathrm{j}\alpha}$ and ensuring that $A \neq 0$ as well as $\alpha \neq \pi/2$, it holds for the ratio of the output signals

$$\frac{y_2}{y_1} = \frac{1 + \mathrm{j}\frac{B}{A}\tan\alpha}{1 - \mathrm{j}\frac{B}{A}\tan\alpha} \,. \tag{6}$$

Comparing (6) with the results in [8], the following relation holds between the design parameters A and B on the one side and the BMAA parameters η and ξ on the other side:

$$\frac{B}{A} = z = \eta + \mathrm{j}\xi \,. \tag{7}$$

This leads to a straightforward design process: After choosing a desired characteristic of the BMAA in terms of an (η, ξ)-pair, the necessary scaling factors A and B can directly be obtained from (7). A and B can be regarded as the transmission factor of a two port which can then be designed accordingly. The number of possible solutions is infinite as several ratios of A and B lead to the same solution. However, some limitations occur as it is highlighted in the following.

When limiting the coupling network to passive components, the absolute values of A and B are limited to values between 0 and 1 as only attenuation and phase shifting can occur. If, e. g., a phase gain $\eta > 1$ is desired, the ratio $|B/A|$ has to be greater than 1. With passive components, this is only possible, if the absolute value of B is significantly greater than the absolute value of A, i. e., A has to be attenuated compared to B. The dependency of the output phase difference curve of A with $B = 1$ is depicted in Fig. 3(a). If an off-boresight characteristic of the BMAA is desired ($\xi \neq 0$), a phase shift has to be introduced between the scaling factors A and B. Its effect is shown in Fig. 3(b) for constant absolute values of $|A| = 0.5$ and $B = 1$ and phase differences of $0°$, $50°$, and $70°$. For the phase shift of $50°$ only a small deviation in the phase difference can be recognized while at $70°$ a significant increase in steepness for incidence angles around $\theta \approx \pm 15°$ can be recognized.

IV. Practical Realization

In order to verify the theoretical concept, a prototype in the E-band around 76 GHz was developed using the new coupling network topology. The placement of two planar rat-race couplers side by side as it is suggested by the flow chart in

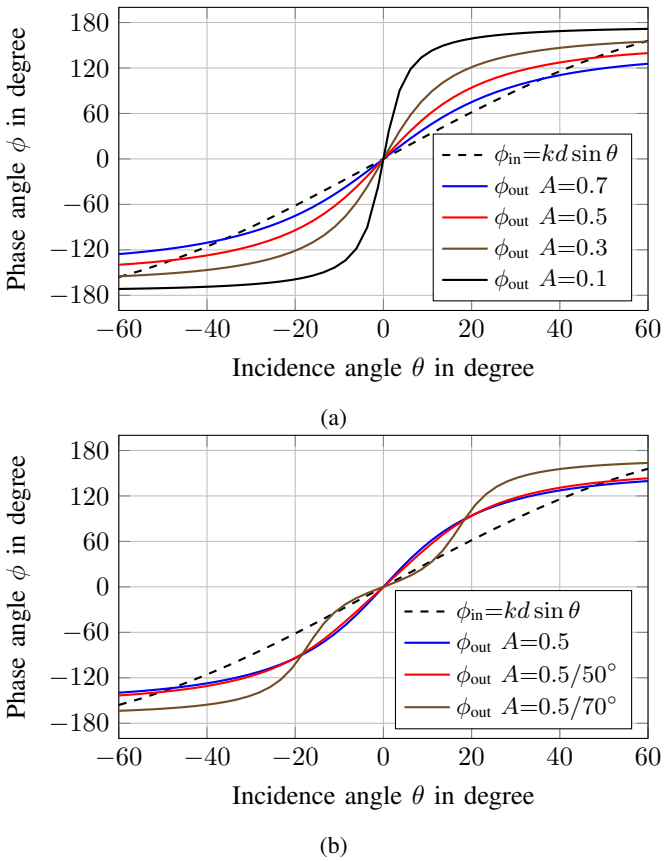

Fig. 3. Variation of the output phase difference ϕ for (a) different real values of A and $B=1$ and (b) different complex values of A and $B=1$.

Fig. 2 is impossible without the need for vias and transitions to other metal layers on the connection lines. To avoid these lossy components and to ensure symmetrical connecting lines between the couplers, the two rat-race couplers were scaled in size and placed inside of each other around the antennas. The inner coupler is connected to the antennas in the center and realizes the addition shown in the first dashed box in Fig. 2. The outer rat-race coupler realizing the addition in the second box takes the scaled signals of common and differential mode and feeds them to its outputs.

A sketch of the complete layout is depicted in Fig. 4. Both couplers have equal microstrip line widths of 0.16 mm in the circle and 0.31 mm on the feed lines. This corresponds to a characteristic impedance of 70.7 Ω and 50 Ω, respectively. The couplers were designed and optimized individually by full-wave simulations on a 127 µm thick RO3003 substrate to ensure a good transmission coeff. and correct transmission phases, respectively. The inner rat-race coupler was designed with a radius of 4.30 mm while the outer one has a radius of 5.53 mm. The two antenna elements are realized as aperture coupled patch antennas on the top layer of a second 127 µm thick RO3003 substrate on top of the first substrate. They have a length of 0.95 mm, a width of 0.7 mm, and are spaced by 1.95 mm (approx. half a wavelength in free space). The coupling slots of the antennas are located in the ground plane

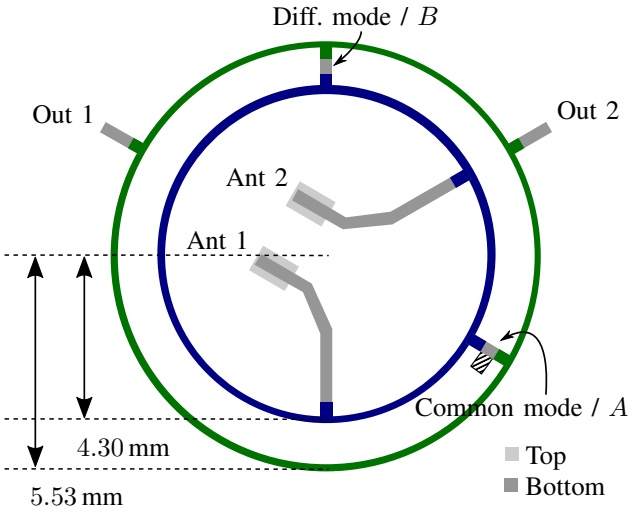

Fig. 4. Layout of the proposed biomimetic coupling network consisting of two interleaved rat-race couplers (bottom view). The inner rat-race coupler is marked blue, the outer one green. An open-ended stub line on the common-mode line—as a complex scaling method realizing A and used in the presented design—is hatched.

between the two substrates.

By connecting the sum and the difference ports of the inner rat-race coupler directly to the inputs of the outer coupler via lines of equal length, no change in output phase difference is observed. This realization is considered as the reference antenna for the measurements and corresponds to the scaling factors $A=B=1$. To realize a specific BMAA behavior, a scaling via A and B is possible. As only passive components are used in this work, the scaling factors A and B can both be chosen in the range between 0 and 1.

In this work, an off-boresight BMAA optimized for an incidence angle of $\theta=\pm10°$ was realized. The calculations in [4] require the BMAA parameters to be chosen to ($\eta=1$, $\xi=3.3$). Therefore, according to (7), the ratio B/A needs to be a complex value. The differential mode scaling factor B is arbitrarily chosen to 1 and, as a consequence, the scaling factor A needs to be realized as

$$A=\frac{1}{1+\mathrm{j}3.3}=0.29\,\mathrm{e}^{-\mathrm{j}\,73.1°}\ . \tag{8}$$

An open-ended stub line with a length of 0.5 mm at the common mode connection line between the two rat-race couplers was chosen as the two-port to realize the scaling. It shows a simulated transmission factor of 0.285 at a phase of −60°. This corresponds to the BMAA parameters ($\eta=1.7$, $\xi=3.0$) which are close to the desired ones. It is important to note that the transmission factor is very sensitive to the length of the stub. A photograph of the manufactured BMAA is shown in Fig. 5.

V. Measurements

The fabricated antenna was measured in an anechoic chamber by using a robotic arm [9]. A horn antenna mounted on the robotic arm was moved on a trajectory around the antenna under test (AUT) at a constant distance of 60 cm.

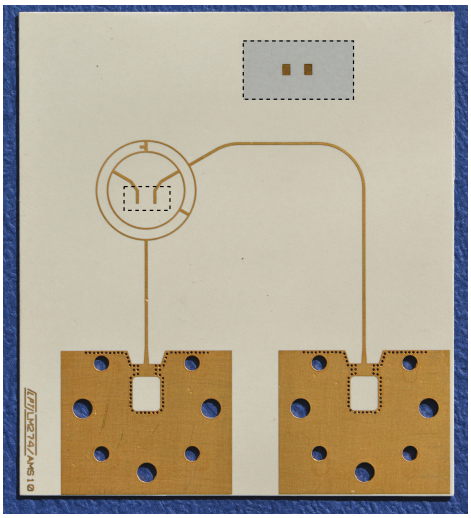

Fig. 5. Photograph of the realized BMAA at 76 GHz (bottom view) with transitions to E-band waveguides. The dashed box shows an enlarged view of the patch antennas on the top layer.

By using a vector network analyzer with external E-band frequency converters, the transmission factor between the AUT and the horn antenna was measured for both of the AUT ports.

Fig. 6(a) shows the measured output phase difference between the two antenna ports for the reference antenna (i. e. $A = B = 1$) and the BMAA as described in Section IV with ($\eta = 1.7,\ \xi = 3.0$), each at 76 GHz. The BMAA shows its maximum angular sensitivity at around $\theta = \pm 10°$ as desired in the design process. Both antenna measurements show a perfect agreement with the theoretically derived curves and thus confirm the underlying theory.

The normalized output power L_{out} of the BMAA is depicted in Fig. 6(b). The measured curves agree well with the analytically predicted ones. A minimum L_{out} of -18 dB is obtained for one port where ϕ_{out} is steepest. This high loss results from the comparably high gain in phase sensitivity of the BMAA around $\theta = \pm 10°$.

VI. Conclusion

A new topology to realize the biomimetic coupling network was presented in this paper. This approach is not dependent on a transformer, which simplifies the use especially in high frequency bands. The influence of the coupling network parameters A and B was demonstrated and the relation to the BMAA parameters η and ξ was derived. A prototype at 76 GHz was developed, fabricated, and measured showing a good match to the analytically predicted behavior.

Acknowledgment

This work was funded by the German Research Foundation (DFG, Deutsche Forschungsgemeinschaft) – WA 3506/6-1.

References

[1] R. N. Miles, D. Robert, and R. R. Hoy, "Mechanically coupled ears for directional hearing in the parasitoid fly Ormia ochracea," *The Journal of the Acoustical Society of America*, vol. 98, no. 6, pp. 3059–3070, Dec. 1995.

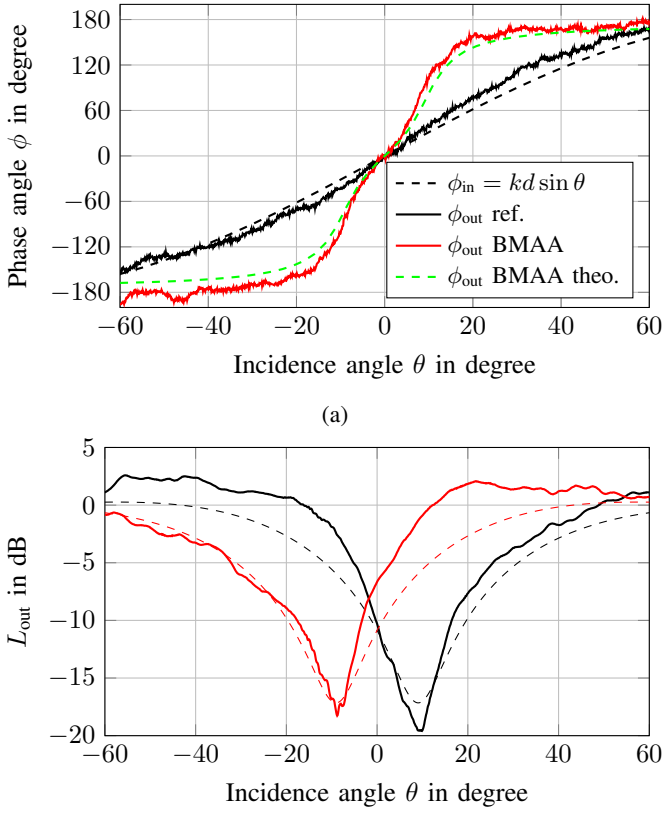

Fig. 6. (a) Measured output phase differences ϕ_{out} for the reference antenna ($A = B = 1$) and the BMAA with parameters $\eta = 1.7$; $\xi = 3.0$ at 76 GHz and (b) theoretical (dashed) and measured (solid) normalized output power L_{out} of port 1 (——) and port 2 (——).

[2] A. R. Masoumi, Y. Yusuf, and N. Behdad, "Biomimetic Antenna Arrays Based on the Directional Hearing Mechanism of the Parasitoid Fly Ormia Ochracea," *IEEE Transactions on Antennas and Propagation*, vol. 61, no. 5, pp. 2500–2510, May 2013.

[3] P. Grüner, T. Chaloun, and C. Waldschmidt, "Towards a mm-Wave Planar Biomimetic Antenna Array with Enhanced Phase Sensitivity," in *10th European Conference on Antennas and Propagation (EuCAP)*, Apr. 2016.

[4] P. Grüner, S. Nguyen, T. Chaloun, and C. Waldschmidt, "Enhancing Angle Estimation for Off-Boresight Targets Using Biomimetic Antenna Arrays," in *48th European Microwave Conference*, Madrid, Sep. 2018.

[5] A. R. Masoumi, K. Ghaemi, and N. Behdad, "A Two-Element Biomimetic Antenna Array With Enhanced Angular Resolution and Optimized Power Extraction," *IEEE Transactions on Antennas and Propagation*, vol. 63, no. 3, pp. 1059–1066, Mar. 2015.

[6] A. M. Elfrgani and R. G. Rojas, "Biomimetic Antenna Array Using Non-Foster Network to Enhance Directional Sensitivity Over Broad Frequency Band," *IEEE Transactions on Antennas and Propagation*, vol. 64, no. 10, pp. 4297–4305, Oct. 2016.

[7] M. R. Nikkhah, K. Ghaemi, and N. Behdad, "An Electronically Tunable Biomimetic Antenna Array," *IEEE Transactions on Antennas and Propagation*, vol. 66, no. 3, pp. 1248–1257, Mar. 2018.

[8] P. Grüner, T. Chaloun, and C. Waldschmidt, "A Generalized Model for Two-Element Biomimetic Antenna Arrays," *IEEE Transactions on Antennas and Propagation*, vol. 67, no. 3, pp. 1630–1639, Mar. 2019.

[9] L. Boehm, F. Boegelsack, M. Hitzler, and C. Waldschmidt, "The Challenges of Measuring Integrated Antennas at Millimeter-Wave Frequencies [Measurements Corner]," *IEEE Antennas and Propagation Magazine*, vol. 59, no. 4, pp. 84–92, Aug. 2017.